Ionics (2008) 14:43–51
DOI 10.1007/s11581-007-0133-8

ORIGINAL PAPER

Electrochemical and impedance spectroscopy studies in H_2/O_2 and methanol/O_2 proton exchange membrane fuel cells

Antonio Rodolfo dos Santos · Marcelo Carmo · Almir Oliveira-Neto · Estevam V. Spinacé · João G. Rocha Poço · Christina Roth · Hartmut Fuess · Marcelo Linardi

Received: 16 February 2007 / Accepted: 28 June 2007 / Published online: 25 July 2007

Abstract This works report results of the structural and the electrochemical characterization of membrane electrode assemblies (MEA) for proton exchange membrane fuel cells (PEMFC) under various cell conditions using different MEA production processes. Electrochemical impedance spectroscopy (EIS) was applied "on-line" (in situ) as a tool for diagnosis concerning the cell performance. MEA with a 25-cm^2 surface area were prepared using Pt/C and Pt–Ru/C commercial electrocatalysts from E-TEK and Pt–Ru/C electrocatalysts produced by the alcohol reduction process. The catalytic ink was applied directly onto the carbon cloth or, alternatively, onto the Nafion® membrane. Two carbon cloth thicknesses were tested as diffusion layers in the MEA: 0.346 mm (common) and 0.424 mm (ELAT). An increase of the electrocatalytic activity can be obtained by pH control in the alcohol reduction process, possibly due to the better particle dispersion and the smaller particle sizes observed. In addition, a slower current decay in the ohmic region was observed using the thinner carbon cloth. This can be related to a lower resistance of the gas flow through the cloth to the catalytic active layer. Different types of methanol feed were employed in the experiments: by humidification and by evaporation. The results showed that the choice of suitable methods for catalyst preparation as well as for MEA production enhance PEMFC performance.

Keywords Pt · Pt–Ru · PEMFC · DMFC · EIS · XRD · TEM · SEM

A. R. dos Santos · C. Roth · H. Fuess
Institute for Materials Science,
University of Technology Darmstadt,
Petersenstrasse 23,
64287 Darmstadt, Germany

A. R. dos Santos (✉) · M. Carmo · A. Oliveira-Neto · E. V. Spinacé · M. Linardi
Fuel Cell Program, Nuclear and Energy Research Institute,
IPEN-CNEN/SP,
Av. Lineu Prestes, 2242, Cidade Universitária,
CEP: 05508-000 São Paulo, SP, Brazil
e-mail: arsantos@ipen.br

J. G. Rocha Poço
Technological Research Institute of São Paulo (IPT),
Av. Prof. Almeida Prado, 532, Cidade Universitária,
CEP: 05508-901 São Paulo, SP, Brazil

Introduction

Proton exchange membrane fuel cells (PEMFC) are suitable for portable, mobile, and stationary applications because of their inherent advantages, such as high-power density, reduced system weight, simple construction, and quick start-up even at low operating temperatures, producing low (or no) emissions [1–3]. For portable and mobile applications, one of the problems is the bulkiness of storage systems for compressed H_2, another one the inefficient storage technologies to date. Furthermore, there is a lack in efficient infrastructure to distribute H_2 to the consumer. An alternative to the use of H_2 as fuel in PEMFC is methanol, which is safer and, as a liquid, offers easy handling, storage, and distribution. Methanol can be directly transformed to electrical current in a direct methanol fuel cell (DMFC). However, the performances currently reached in a DMFC are far from ideal when compared with a PEMFC. The decrease of the cell performance is due to the carbon monoxide (CO) formed in the oxidation of methanol, which

adsorbs irreversibly on the Pt surface. To reduce the poisoning, a second metal supplying oxygenated species at potentials significantly lower than those for pure Pt is added [4]. Another major problem is fuel crossover in the DMFC, impacting system efficiency by the formation of a mixed potential at the cathode and avoidable loss of fuel [4–6].

A possibility to reduce methanol crossover during the operation of the cell would be either to use thicker and less permeable membranes or different gas diffusion layers (GDL) in the production of MEA. However, thicker membranes and backings are usually avoided, as they show an inherently higher resistance along with a less efficient removal of gaseous products [6, 7]. Lu and Wang [8] studied the effect of the formation of CO_2 bubbles at the anode of the cell. The authors correlated the decreasing cell performance with the difficult removal of gaseous products resulting in severe mass transport limitations. To improve the removal of the CO_2 bubbles, the authors researched alternatives to Toray™ paper commonly used as GDL in the production of MEA. In their study, hydrophilic carbon cloth backings without previous treatment showed better performances and more effective removal of gaseous products than the hydrophobized Toray™ with a wet-proof treatment of 2 $mg \cdot cm^{-2}$ Teflon. However, with respect to the H_2O formation at the cathode and water management in the fuel cell, the use of Toray™ paper gave better results than the hydrophilic carbon cloth because the removal of the water excess was facilitated. Although other researchers [9, 10] used carbon cloth ELAT in their MEA production, no in-depth study of alternative backings has been reported so far.

One of the alternatives to improve cell performance would be a significant reduction of the MEA ohmic resistance. This approach was studied by Frey and Linardi [2], comparing two methods for painting the catalytic layer: directly onto the membrane or onto the GDL. Using electrochemical impedance spectroscopy (EIS), they found a reduced ohmic resistance of the MEA when the catalytic layer is painted directly on the carbon cloth. Up to now, the detailed reasons for this improvement are not yet clear and need further investigations by systematic microstructure analysis.

However, not only the MEA preparation process but also the catalyst preparation needs to be optimized to achieve high fuel-cell performances required. The electrocatalyst preparation should aim at a better nanoparticle distribution on the support and smaller particle sizes. In the literature, numerous efforts involving the electrocatalysts preparation have been reported, ranging from simple reductive precipitation methods [11, 12] to the more elaborate colloid [13–15] and microemulsion methods [16, 17]. A simple and inexpensive way to obtain high quality electrocatalysts is the alcohol reduction process [18–22]. Among these studies, Wang and Hsing [18] prepared Pt/C and Pt–Ru/C catalysts from alcohol reduction process with particles sizes in the range of 2.0–3.5 nm and a performance comparable to the commercial E-TEK electrocatalyst.

In the work presented, commercial and in-house synthesized Pt–Ru/C catalysts were characterized structurally and electrochemically. Particle size, structure, and particle distribution on the support were assessed by X-ray diffraction (XRD) and transmission electron microscopy (TEM). The electrocatalytic properties were determined in current–voltage curves and by EIS. Two types of diffusion layer (common and ELAT) were tested and two types of MEA preparation by either painting on the backing or the membrane.

Experimental

Pt–Ru/C electrocatalysts prepared by alcohol reduction process

Pt–Ru/C electrocatalysts (20 wt%, Pt/Ru atomic ratio of 1:1) were prepared (with or without pH control) using ethylene glycol (Merck) as solvent and reducing agent, $H_2PtCl_6 \cdot 6H_2O$ (Aldrich) and $RuCl_3 \cdot xH_2O$ (Aldrich) as metal sources, and high surface area Carbon Vulcan XC-72R as support. More details on the preparation procedure using this methodology can be found in previous publications [20–22]. During the catalyst preparation with pH control, the pH of the reaction medium was kept at 11 by addition of KOH solution (1 mol l^{-1}). Pt/C (20 wt%) and Pt–Ru/C (20 wt%, Pt/Ru atomic ratio of 1:1) commercial electrocatalysts from E-TEK were used for comparison.

Table 1 Pt/Ru atomic ratio and mean particle sizes of the prepared electrocatalysts

Electrocatalysts		Nominal atomic ratio (%)		Atomic ratio–EDX (%)		Particle size[a] (nm)	Particle size[b] (nm)
		Pt	Ru	Pt	Ru		
Alcohol reduction synthesis	Pt–Ru/C	50	50	52	48	2.5	2.8
	Pt–Ru/C pH=11	50	50	50	50	0.9	2.0
Commercial	Pt–Ru/C E-TEK	50	50	47	53	2.1	1.8
	Pt/C E-TEK	–	–	–	–	2.1	2.0

[a] Mean particle size calculated from X-ray diffraction data using the Scherrer equation.
[b] Mean particle size calculated using the TEM images.

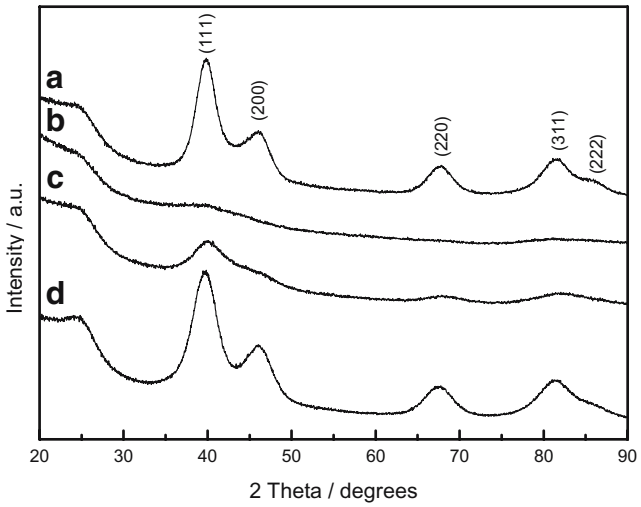

Fig. 1 X-ray diffractograms of the different electrocatalysts: *a* Pt–Ru/C alcohol reduction process, *b* Pt–Ru/C alcohol reduction process at pH=11, *c* Pt–Ru/C E-TEK, and *d* Pt/C E-TEK

The Pt/Ru atomic ratios of the electrocatalysts were determined using a scanning electron microscope (SEM) Philips XL30 with a 20-keV electron beam and equipped with EDAX DX-4 microanalyses. The XRD analyses were performed using a STOE STADI-P diffractometer with germanium monochromized Cu Kα radiation and a position-sensitive detector with 40° aperture in transmission mode. Particle sizes were determined from X-ray patterns using the Scherrer equation [23] and manually from the transmission electronic microscopy (TEM) images using a Philips CM20 UT with 200 kV.

Catalyst ink preparation

Pt–Ru/C and Pt/C electrocatalysts were used to prepare the electrode precursor inks. Millipore water was added to the electrocatalyst in a weight ratio of 25:1. The ink was stirred in a one-tip ultrasonic mixer. Then a water-based 10 wt% Nafion® solution from DuPont (SE-10072) was directly added to the electrocatalyst/water slurry. The Nafion® content in the dry electrodes was 35.8 wt%. Finally, the ink was stirred with a magnetic stirrer during 24 h, resulting in homogeneous distribution of the Nafion® ionomer in the solution.

MEA and single-cell operation

Nafion® 105 (DuPont) polymer electrolyte membranes were used in the experiments. These membranes were treated with 3 wt% H_2O_2 during 1 h at boiling point, cleaned with 100 °C hot Millipore water, treated with 1 mol

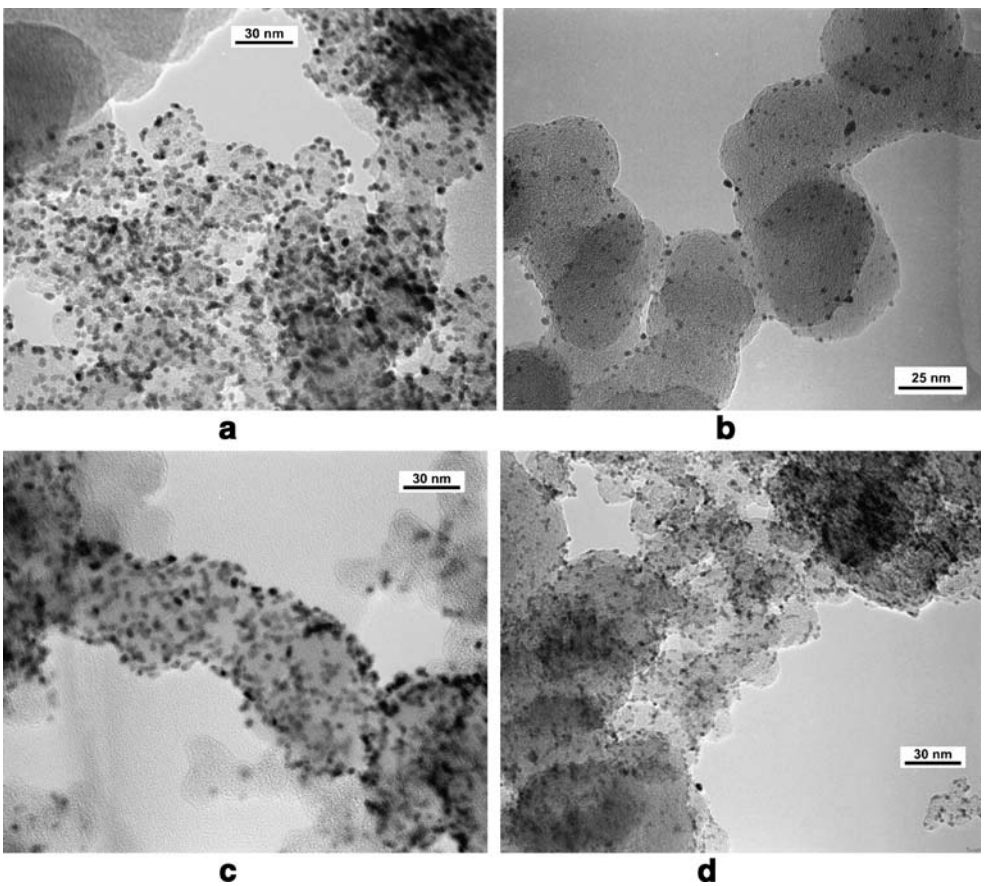

Fig. 2 TEM micrographs of the electrocatalysts with Pt/C and Pt–Ru/C by alcohol reduction process with and without pH control: **a** Pt/C with pH control, **b** Pt/C without pH control, **c** Pt–Ru/C with pH control, and **d** Pt–Ru/C without pH control

l^{-1} H_2SO_4 during 1 h at boiling point and cleaned with 100 °C, hot Millipore water again.

An aluminum frame was used to fix the Nafion membrane or the GDL, depending on the side used to receive the catalyst ink. After drying, the frame was placed on a vacuum-heating table at 125 °C and weighed regularly until constant weight. An airbrush gun was used for catalyst application. The catalyst ink was sprayed in layers directly onto the membrane or onto the GDL. Again, the weight was controlled by regular measurements after each sprayed layer was dried. The noble metal concentrations used were set to 0.4 mg Pt cm^{-2} at the anode (Pt/C and Pt–Ru/C 20 wt%) and 0.6 mg Pt cm^{-2} at the cathode (Pt/C 20 wt% only E-TEK). The MEA were pressed together with gas diffusion layers at 125 °C, 5 tons for 2 min [24]. Two types of GDL were used in this work, common carbon cloth (0.346-mm thickness) and carbon cloth ELAT (0.424-mm thickness), with a Teflon loading of 35 wt%.

The MEA were put in a graphite single cell with punctual flow field (25-cm^2 single cell ElectroChem). After conditioning the cell for 2 h at a constant cell potential of 600 mV, polarization curves were measured. The experiments with H_2/O_2 were performed with humidified H_2 (T_{hum}=80 °C) and dry O_2 at a cell temperature of 65 °C with ambient pressure on the anode and cathode side. Regarding the experiments with methanol/O_2, two different alcohol feeding devices were investigated: (1) vaporizer—methanol (2 mol l^{-1}) was pumped from a container with a peristaltic pump into a quartz vaporizer maintained at 130 °C at a cell temperature of 85 °C and dry O_2, (2) humidifier—the experiments with humidified methanol (2 mol L^{-1}) were carried out using a humidifier (T_{hum}=95 °C) at a cell temperature of 85 °C and dry O_2. For all experiments, the flow of oxygen and hydrogen was kept constant at 50% over the whole current density range.

A Dynaload (TDI model RBL 488) was used as electronic load for the polarization curve measurements. For the EIS measurements used, a FC350 fuel cell EIS System (GAMRY) was used coupled to a PC4 potentiostat/galvanostat and the system connected to the electronic load (TDI) for on-line EIS experiments (100 mHz–10 kHz, dU= 5 mV).

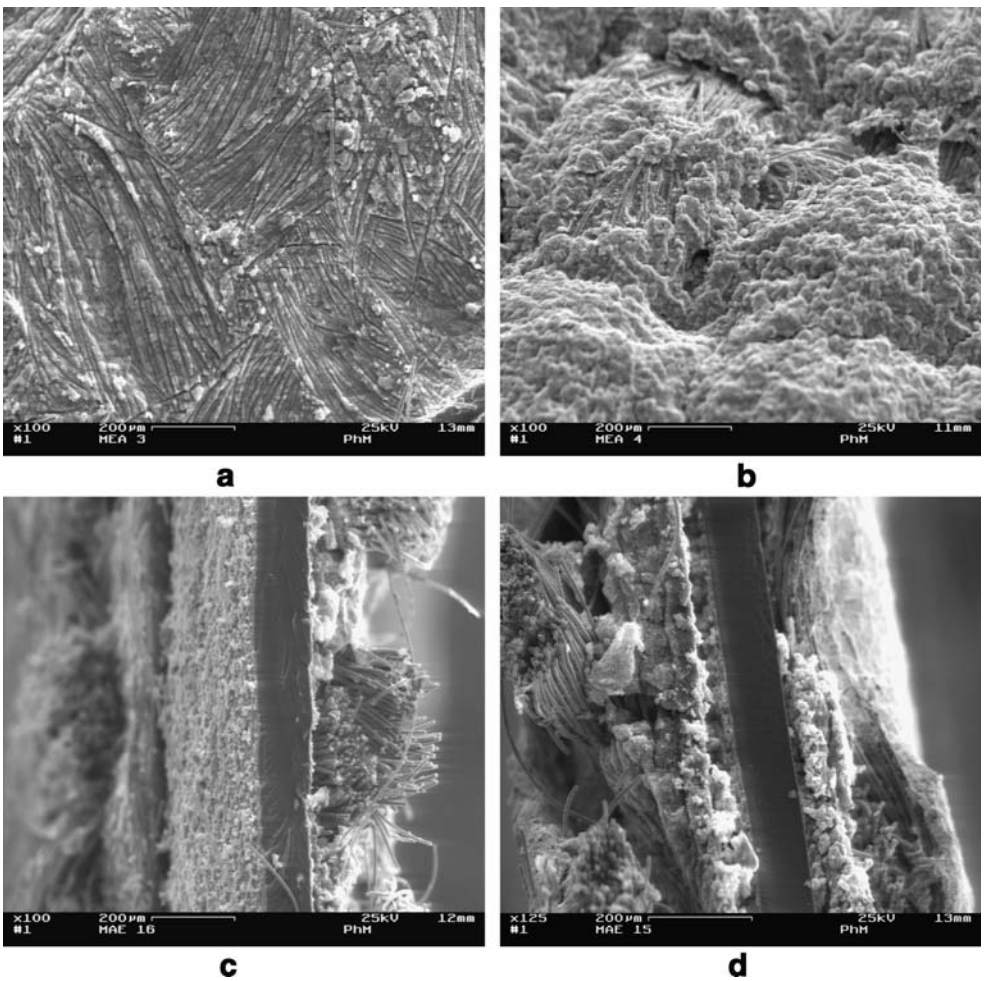

Fig. 3 SEM micrographs of the MEA with Pt/C E-TEK in **a** common carbon cloth printed onto the membrane, **b** common carbon cloth printed onto the carbon cloth, **c** carbon cloth ELAT printed onto the membrane, and **d** carbon cloth ELAT printed onto the carbon cloth

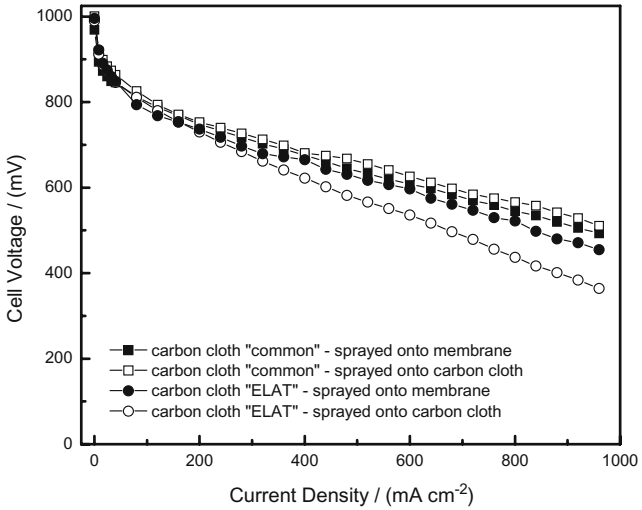

Fig. 4 Polarization curves of MEA with 25 cm^2 active surface area, manufactured with Pt/C E-TEK 20% with 0.4 mg cm^{-2} at the anode and 0.6 mg cm^{-2} at the cathode, operating with H_2/O_2. Temperatures: cell 65 °C and humidifier 85 °C

Results and discussion

Pt–Ru/C electrocatalysts characterization prepared by the alcohol reduction process

The EDX analysis and the mean particle sizes of the electrocatalysts are shown in Table 1.

The Pt/Ru atomic ratios of the electrocatalysts prepared by the alcohol reduction process were in good agreement with the nominal atomic ratios. The average particle size, D, may be estimated according to the Scherrer equation [23], as summarized in Table 1.

$$D = \frac{0.9\lambda_{k_{\alpha 1}}}{B_{(2\theta)}\cos\theta_{\max}} \quad (1)$$

where the radiation wavelength $\lambda_{k_{\alpha 1}}$ is 1.54056 Å, and the reflection width $B_{(2\theta)}$ is in radians.

The average particle sizes were in the range of 2.5 nm for Pt–Ru/C electrocatalysts, while a decrease in the particle sizes was observed for the Pt–Ru/C formulation synthesized with pH=11, which was induced by increasing the pH of the solution.

The X-ray diffraction patterns of the electrocatalysts are displayed in Fig. 1. The electrocatalysts showed the characteristic peaks corresponding to the fcc structure of platinum and platinum alloys at 2θ=40, 47, 67, and 82° [25–27]. The broad peak at 2θ=25° was associated with the Vulcan XC 72R support material. No other peaks of ruthenium hcp phase or ruthenium oxides were observed. However, Ru or Ru oxides might be present as particles smaller than 2 nm in size or in amorphous form, which then could not be detect by X-ray diffraction.

TEM micrographs of the Pt/C electrocatalysts prepared by the alcohol reduction process at pH=11 (Fig. 2a) reveal nanoparticles, with an average particle size of 2.9 nm, homogenously distributed over the carbon surface. For the Pt/C without pH control (Fig. 2b), the nanoparticles distribution over the carbon surface was found to be considerably less homogeneous, and particle sizes are 2.5 nm. Pt–Ru/C electrocatalysts prepared by the alcohol reduction process at pH=11 (Fig. 2c) show a relatively uniform nanoparticles distribution on the carbon surface and have particle sizes in the range of 2.0 nm. In comparison, for Pt–Ru/C without pH, the nanoparticle distribution is not relatively uniform on the carbon surface (Fig. 2d), and the obtained particle sizes are in the range of 2.8 nm.

The SEM micrographs of the MEA with the common carbon cloth are shown in Fig. 3a (printed onto the membrane) and b (printed onto the carbon cloth). The MEA with carbon cloth ELAT are shown in Fig. 3c (printed onto the membrane) and d (printed onto the carbon cloth). It

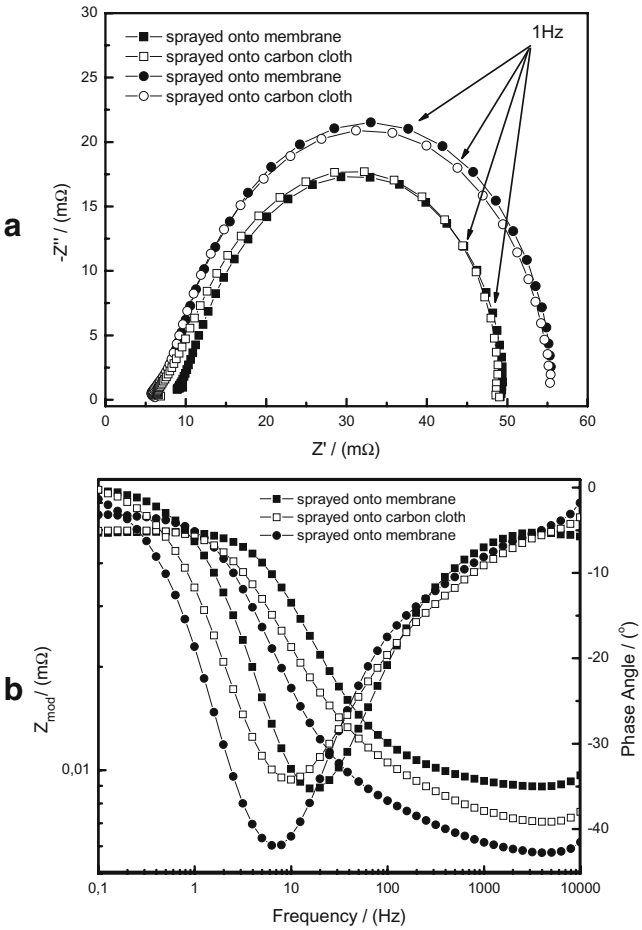

Fig. 5 Nyquist diagrams (**a**) and Bode diagrams (**b**) for MEA with 25 cm^2 of active surface area, manufactured with Pt/C E-TEK 20% with 0.4 mg cm^{-2} at the anode and 0.6 mg cm^{-2} at the cathode, operating with H_2/O_2 at 1.0 A. *Square* symbols represent common carbon cloth and *round* symbols carbon cloth ELAT. Temperatures: cell 65 °C and humidifier 85 °C

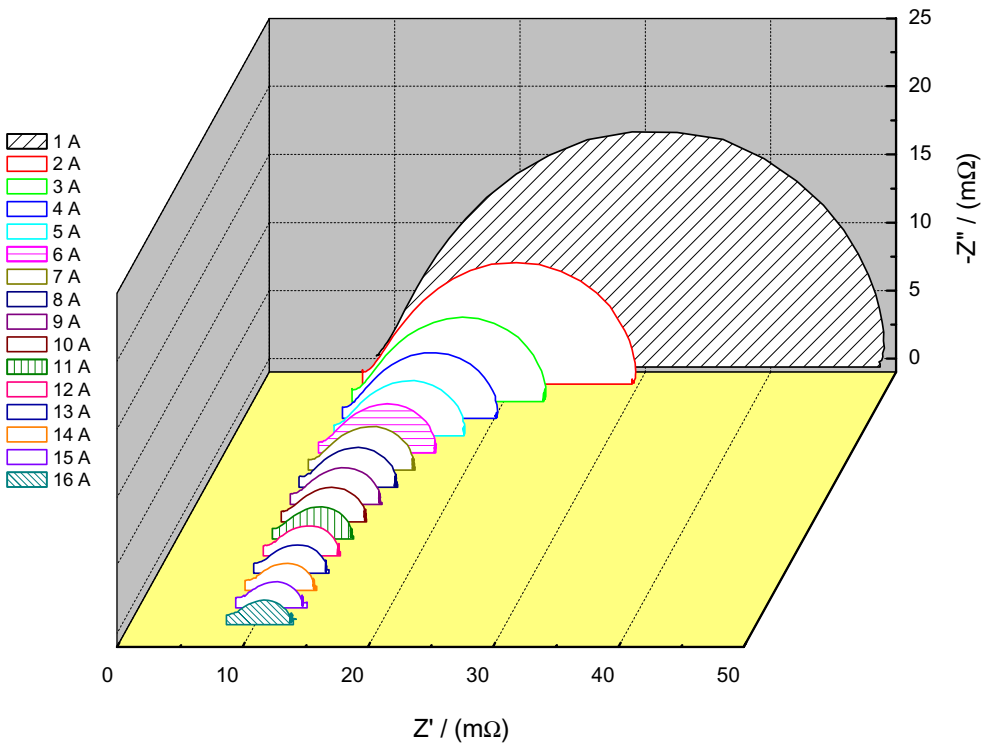

Fig. 6 Nyquist diagrams for MEA with 25 cm^2 of active surface area, manufactured with Pt/C E-TEK 20% painted on common carbon cloth with 0.4 mg cm^{-2} at the anode and 0.6 mg cm^{-2} at the cathode, operating with H_2/O_2 between 1.0 and 16.0 A. Temperatures: cell 65 °C and humidifier 85 °C

can be observed that the painting methods onto the membrane as well as onto the carbon cloth show good electrode layer homogeneity. However, when the ink was painted onto the carbon cloth, the catalytic ink permeates the fibers of the carbon cloth, increasing the electrode active area. Such effect is more noticeable for the common carbon cloth because this material presents a larger space among the carbon cloth fibers. In addition, the ELAT possesses an intrinsic diffusion layer, hindering ink permeation.

Electrochemical results

Two carbon cloth thicknesses were tested as gas diffusion layer in the MEA: 0.346 mm (common) and 0.424 mm (ELAT). Figure 4 displays the polarization curves corresponding to MEA with the different carbon cloths, manufactured with Pt/C (E-TEK) electrocatalyst and operating with H_2/O_2.

The results obtained using the common carbon cloth, exhibit a slower current decay in the ohmic region. This feature can be related to a lower gas flow resistance through the cloth to the catalytic active layer, probably due to the lower degree of interlacement of this carbon cloth. Furthermore, it is shown that, by painting the catalytic ink directly onto the common carbon cloth, a higher current density is obtained when compared with painting directly onto the membrane (680 to 640 mA at 598 mV, respectively). This might be explained by the MEA painting procedure, where the membrane was kept quite a long time on the vacuum table (130 °C, as the catalytic ink contains water as a solvent), drying up the membrane. This painting procedure might result in a severe drying and incomplete rehumidification of the membrane. Another fact can also be related to the water contained in the ink, which spreads better on the surface of the carbon cloth (due to the hydrophobic properties of the Teflon). However, it is observed that using the carbon cloth ELAT, an increase in current values is observed when the ink was painted onto the membrane. This can be due to the formed electrocatalyst agglomerates when painting directly onto the

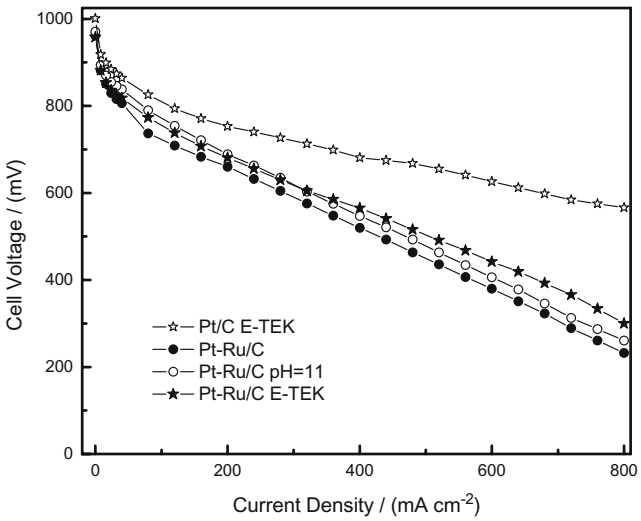

Fig. 7 Polarization curves of MEA with 25 cm^2 active surface area, manufactured with Pt–Ru/C 20%, using the alcohol reduction process with and without pH control, 0.4 mg of Pt cm^{-2} at the anode and 0.6 mg of Pt cm^{-2} at the cathode, operating with H_2/O_2. For comparison, curves of the MEA manufactured with Pt/C and Pt–Ru/C E-TEK painted onto the carbon cloth are displayed. Temperatures: cell 65 °C and humidifier 85 °C

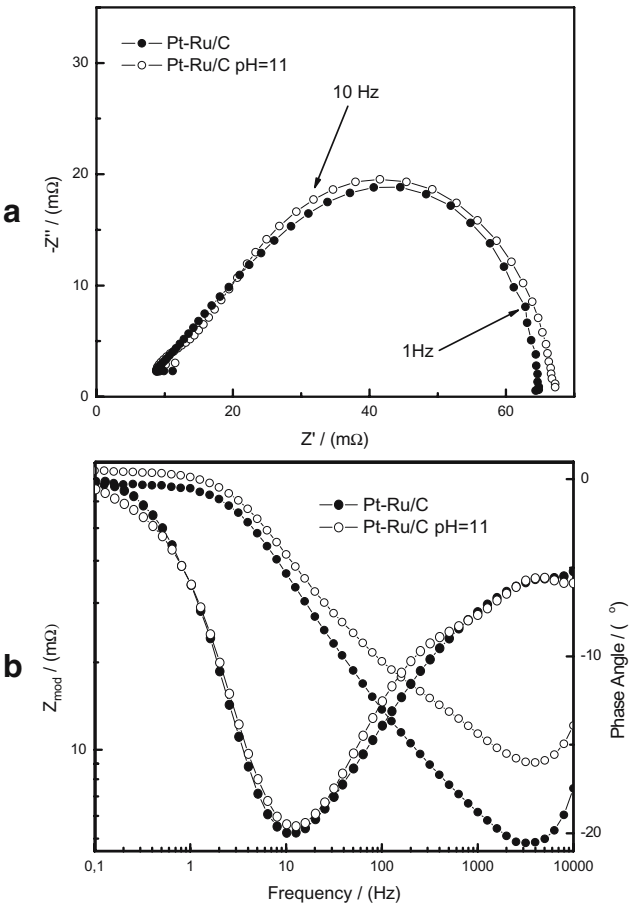

Fig. 8 Nyquist diagrams (**a**) and Bode diagrams (**b**) for MEAs with 25 cm^2 active surface area, manufactured with Pt–Ru/C 20%, alcohol reduction process with and without pH control, 0.4 mg of Pt cm^{-2} at the anode and 0.6 mg of Pt cm^{-2} at the cathode, operating with H_2/O_2 at 1.0 A. Temperatures: cell 65 °C and humidifier 85 °C

carbon cloth ELAT (well interlaced, different from the common one, where the ink is crossed among the mesh).

In Fig. 5, Nyquist (a) and Bode (b) diagrams are shown for MEA with the different carbon cloth manufactured with Pt/C E-TEK, operating with H_2/O_2 at 1.0 A. From the analysis of the Nyquist diagrams of Fig. 5a, it is observed that the MEA manufactured with carbon cloth ELAT exhibit a higher ohmic resistance (the ohmic resistance was obtained from the high frequency intercept with the *Z*′-axis) in relation to the MEA with common carbon cloth. This can be related to the stronger interlacement of the mesh of this carbon cloth ELAT and, along with the thickness influence, result in higher resistances to gas diffusion after the painting procedure. It can be observed that the MEA using carbon cloth ELAT and painted onto the membrane exhibits a higher resistance than the MEA painted directly onto the carbon cloth ELAT.

In the Bode diagrams of Fig. 5b, the value of impedance for the high phase angle (the so-called inflection impedance) and the corresponding frequency are correlated with two different kinetic electrochemical phenomena of the cathodic and anodic reactions [28]. This phase angle is directly related to the resistive and capacitive effect in the cell: the smaller the value of the phase angle, the smaller the resistive effect of the MEA. Observing the Bode diagrams of Fig. 5b, for the MEA with common carbon cloth painted directly onto the carbon cloth, a smaller phase angle was found, as expected. Therefore, this MEA shows low resistance. The MEA painted onto the membrane using the carbon cloth ELAT exhibited an excessively high-phase angle, also presenting a high resistance in the Nyquist diagram.

In Fig. 6, Nyquist diagrams are shown concerning the MEA manufactured with Pt/C E-TEK, operating with H_2/O_2 under various operation currents. Analyzing these Nyquist diagrams, one can conclude that the MEA resistance is directly correlated to the cell operation current. The higher the operation current, the lower is the MEA resistance. It is also observed that, for currents up to 6.0 A, the measured resistances increase exponentially, and for higher currents, a linear behavior is observed. A similar trend is exhibited in the polarization curve shown in the Fig. 7 for Pt/C E-TEK, where the potential increases exponentially at low current values and linearly at high current values. By comparing the ohmic resistance of the MEA working at 16.0 and 1.0 A, an increase from 13.4 to 49.1 mΩ is evaluated. As a potential around 700 mV is usually considered for practical applications, a resistance value of 15.2 mΩ is estimated at this cell potential.

In Fig. 7, polarization curves of MEA prepared with different electrocatalysts operating with H_2/O_2 are shown. For the electrocatalysts prepared by the alcohol reduction process, the ink was applied directly onto the carbon cloth

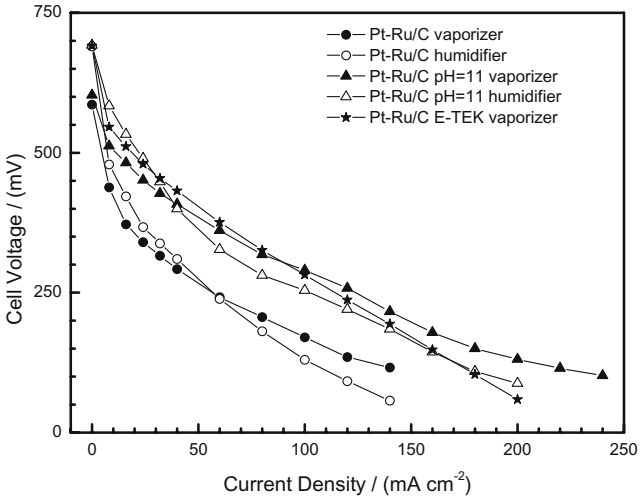

Fig. 9 Polarization curves of MEA with 25 cm^2 active surface area, manufactured with Pt–Ru/C 20%, using the alcohol reduction process with and without pH control, 0.4 mg of Pt cm^{-2} at the anode and 0.6 mg of Pt cm^{-2} at the cathode, operating with methanl/O_2. Temperatures using the vaporizer: cell 85 °C and vaporizer 130 °C. Temperatures using the humidifier: cell 85 °C and humidifier 95 °C

only on the anode side. The cathode was sprayed with Pt/C E-TEK. For the MEA represented by open symbols in Fig. 7, the pH of the reaction medium was kept at 11, while for the MEA represented by full symbols, the pH was not modified. For comparative purposes, polarization curves for MEA manufactured with Pt/C and Pt–Ru/C E-TEK sprayed on carbon cloth were presented. With pH control during the electrocatalysts preparation, a small increase in cell potential was obtained due to the better homogeneity of the Pt–Ru particles anchored in the carbon surface and/or due to a decrease of the average particle size.

It can also be observed in Fig. 7, at low current densities, that there is a significant performance difference between the electrocatalysts from E-TEK and those prepared with the alcohol reduction process. A decrease in the activity is more severe for systems without pH control, as the Pt–Ru/C catalysts system, pH=11, shows a negative slope of only 9 mA cm^{-2} for 600 mV, whereas without pH control, a negative slope of 51 mA cm^{-2} for 600 mV has been observed concerning Pt–Ru/C E-TEK.

In Fig. 8, the Nyquist (a) and Bode (b) diagrams of the same MEA described in Fig. 7 are shown under H_2/O_2 cell operation. In the Nyquist diagram, the MEA with Pt–Ru/C with and without pH control showed essentially the same ohmic resistance. This fact can be explained by suppression of agglomerates during the MEA preparation process or by the homogeneity of the anchored electrocatalysts at the carbon surface. This result is in contrast to the polarization curves of the Pt–Ru/C catalysts with and without pH control. The Bode diagrams of Fig. 8b show similar behavior for the phase angle.

MEA polarization curves are shown in Fig. 9, operating directly with 2 mol l^{-1} methanol solution as fuel. The cell temperature and the methanol vaporizer were 85 and 130 °C, respectively. For all the experiments using the humidifier, the cell temperature was 85 °C and the humidifier was 95 °C. For methanol operation, the cell performance is much lower than that for hydrogen operation, for example, at 300 mV, the cell potential is 93 mA cm^{-2} for Pt–Ru/C pH=11 with methanol and 740 mA cm^{-2} with hydrogen operation. Furthermore, using the humidifier below 12 mA cm^{-2} proved to be advantageous, while for higher current densities, the potentials reached are higher for the vaporizer set-up. The pH control in Pt–Ru/C synthesis using the alcohol reduction process showed to have a positive effect, possibly due to the better particle dispersion and the smaller particles sizes.

Another point observed is that the potentials reached for MEA produced with Pt–Ru/C pH=11 electrocatalyst showed the best performance of all. One explanation to this effect is that, controlling the pH of the reaction medium by the electrocatalysts preparation, a better Pt–Ru dispersion on carbon surface and smaller particle sizes were reached.

Conclusion

The results presented show that a beneficial increase of the electrocatalytic activity can be obtained if a suitable catalyst synthesis process is used. The pH control in Pt–Ru/C synthesis using the alcohol reduction process showed a positive effect, possibly due to the better particle dispersion and the smaller particle sizes.

For the results with the common carbon cloth (thinner), a slower current decay in the ohmic region was observed compared to the ELAT carbon cloth (thicker). This can be related to a lower resistance of the gas flow through the cloth reaching the active catalytic layer due to the low degree of interlacement of this carbon cloth. Another remarkable observation was that the electrocatalyst ink, painted on the common carbon cloth, presented a good homogeneity and increased the active electrode area due to larger space among the fibers of the carbon cloth. Another advantage observed was the low gas flow resistance of the cloth due to the low degree of interlacement of this material.

For operations with H_2/O_2, one can also observe that there is a significant difference between the electrocatalysts from E-TEK and those prepared with the alcohol reduction process. Another performance difference was observed between the electrocatalysts prepared by the alcohol reduction process, with and without pH control. A decrease in the activity is more severe for systems without pH control.

Using the vaporizer for the cell operation with methanol/O_2, a better cell performance was observed, comparing with the experiments using the humidifier.

The electrocatalysts prepared by pH=11 solutions presented a higher current density than the process without pH control. Pt–Ru/C electrocatalyst (pH=11) showed the best performance. One possible explanation to this effect is that, controlling the pH of the reaction medium by the electrocatalysts preparation, a better Pt–Ru dispersion on the carbon surface and small particle sizes were obtained.

Acknowledgment The authors wish to thank FAPESP, CAPES, DAAD, CTPETRO/FINEP, IPEN, IPT, and University of Technology Darmstadt, for financial and technical support.

References

1. Wendt H, Götz M, Linardi M (2000) Quím Nova 23:538
2. Frey T, Linardi M (2004) Electrochim Acta 50:99
3. Franco EG, Oliveira-Neto A, Aricó E, Linardi M (2002) J Braz Chem Soc 13:516
4. Camara GA, Giz MJ, Paganin V, Ticianelli EA (2002) J Electroanal Chem 537:21
5. Ren X, Zelenay P, Thomas S, Davey J, Gottesfeld S (2000) J Power Sources 86:111
6. Heinzel A, Barragan VM (1999) J Power Sources 84:70
7. Narayanan SR, Frank H, Jeffries-Nakamura B, Smart M, Chun W, Halpert G, Kosek J, Cropley C (1995) In: Gottesfeld S, Halpert G,

Landgrebe A (eds) Proton conducting membrane fuel cells I, PV 95-23. The Electrochemical Society Proceedings Series, Pennington, NJ, p 278
8. Lu GQ, Wang CY (2004) J Power Sources 134:33
9. Sun X, Li R, Villers D, Dodelet JP, Désilets S (2003) Chem Phys Lett 379:99
10. Qi Z, Kaufman A (2003) J Power Sources 113:37
11. Bittins-Cattaneo B, Iwasita T (1987) J Electroanal Chem 238:151
12. Frelink T, Visscher W, van Veen JAR (1994) Electrochim Acta 39:1871
13. Zhou Z, Wang S, Zhou W, Wang G, Jiang L, Li W, Song S, Liu J, Sun G, Xin Q (2003) Chem Commun 394
14. Franco EG, Oliveira-Neto A, Spinacé EV, Linardi M, Martz N, Mazurek M, Fuess H (2005) Mater Res 8:117
15. Bonnemann H, Brijoux W, Brinkmann R (1991) Angew Chem Int Ed Engl 30:1312
16. Pileni MP (1997) Langmir 13:3266
17. Xiong L, Manthiram A (2005) Electrochim Acta 50:2323
18. Wang X, Hsing I-M (2002) Electrochim Acta 47:2981
19. Zhou W, Zhou Z, Song S, Li W, Sun G, Tsiakaras P, Xin Q (2003) Appl Catal B Environ 46:273
20. Spinace EV, Oliveira-Neto A, Vasconcelos TRR, Linardi M (2004) J Power Sources 137:17
21. Oliveira-Neto A, Vasconcelos TRR, Da Silva RWRV, Linardi M, Spinace EV (2005) J Appl Electrochem 35:193
22. Spinace EV, Oliveira-Neto A, Vasconcelos TRR, Linardi M (2003) Brazilian Patent INPI-RJ, PI0304121-2
23. Scherrer P (1918) Nach Ges Wiss 26:98
24. Linardi M, Baldo WR, Bueno SAA, Saliba-Silva AM (2003) Método híbrido de spray e prensagem a quente, Patent submitted for deposit at INPI Brazil
25. Roth C, Martz N, Fuess H (2001) Phys Chem Chem Phys 3: 315
26. Roth C, Goetz M, Fuess H (2001) J Appl Electrochem 31:793
27. Roth C, Martz N, Fuess H (2004) J Appl Electrochem 34:345
28. De Melo AG (2003) Personal Communication, IQ/USP São Paulo